ZIBELINE INTERNATIONAL PUBLISHING

Acta Mechanica Malaysia (AMM)

DOI : *http://doi.org/10.26480/amm.2.2019.20.27*

ISSN: 2616-4302 (Online)
CODEN : AMMCFL

RESEARCH ARTICLE

EVALUATING THE IMPACT OF UNSTEADY VISCOUS FLOW AND PRESENCE OF SOLID PARTICLES ON PIPELINE SURFACES DURING CRUDE OIL TRANSPORT USING COMPUTATIONAL FLUID DYNAMICS ANALYSIS

Chukwugozie Jekwu Ejeh [1]*, Gbemisola Precious Akhabue[2], Chigozirim Cyprian Onyekperem[3], Evans Boah Annan[1] and Kingsley Kwaah Tandoh[1]

[1]All Nations University College, Eastern Region, Ghana
[2]Presbyterian University College, Eastern Region, Ghana
[3]Center of Excellence in Marine and Offshore Engineering, Rivers State University, Nigeria.
**Corresponding Author E-mail: echukwugozie@gmail.com*

ARTICLE DETAILS

Article History:

Received 27 June 2019
Accepted 29 July 2019
Available online 10 August 2019

ABSTRACT

Pipelines are commonly used in the petroleum industry to extract and transport crude oil and natural gas from the petroleum reservoir to storage facilities. The flow kinematics of crude oil through pipelines is unsteady and is associated with a constant change in the viscosity of fluid. The effect of unsteady viscous flow is predominant at wall boundaries, where there exist relative motion between crude oil and pipe wall, acting in reverse direction. This fluid-wall interaction induces viscous drag at the wall boundary due to friction. When friction occurs, stress and heat will be exerted at the contact interface. Solid particles sourced from the unconsolidated nature of sandstone lithology are transported alongside with crude oil. These particles impinges on the pipe wall and erodes the corrosion resistant layer, thereby exposing the pipe surface to the corrosive fluid. This study is aimed at evaluating the impact of unsteady viscous flow and presence of solid particles on pipeline surfaces during crude oil transport. Identified areas with high viscous stress is important and this was achieved using CFD. The two equation k-ω turbulent model and particle tracing were used as the flow physics, to achieve the aim of this paper. It was established that the properties of crude oil had an influence on the estimation of wall viscosity and erosion rate. The numeric value of the selected fluid properties such as dynamic viscosity, specific gravity, and velocity was in the range 0.08 - 0.20 Pas, 0.66 – 0.93 and 20 – 60 m/s respectively. Regions with maximum contact with the moving fluid had the maximum viscous drag and frictional velocity predictions. This region was identified as the potential hotspot and located at the pipe elbow.

KEYWORDS

Unsteady viscous flow; Erosion rate; Crude oil transport.

1. INTRODUCTION

The increasing demand for energy from fossil fuel to power automobile engines, industrial equipment and heating homes, has led to the rapid development of technologies to produce oil and gas efficiently [1]. Pipelines are commonly used to extract and transport crude oil from the reservoir to its depot site for processing. Flow in pipes can be laminar, translational or turbulent and this regime depends on Reynold's number [7, 8, 9].

Fluid flow through pipes experience a turbulent flow regime, and the degree of turbulence depends mainly on the fluid velocity, density and viscosity. When these parameters are altered, the flow behaviour and interaction with the pipe wall changes [7, 10]. In the modelling of fluid flow through pipes using CFD approach, the two equation $k-\omega$ is used to predict flow features accurately at sensitive areas such as the wall boundaries. This is because, at the wall boundary, there exist an attractive force in the form of interfacial tension, which act at the fluid-wall interface. This force gives birth to a rise in frictional velocity and contributes to an increase in the flow resistance offered by the wall. This anomaly is described as wall viscosity, and the degree of flow resistance can be estimated using this measurable parameter.

It has been established from literature that, sensitive fluid properties such as velocity, density and viscosity contribute to the nonlinear viscous flow behavior experienced during crude transport [7, 13]. This nonlinearity, is the cause of unsteady wall viscosity and its effect is predominantly experienced at areas closest to the pipe curvature [15, 16]. The key objective of this paper is to identify these hotspot areas for different sensitive fluid flow parameters, and also considering the rate of erosion by the contaminant particles.

In this work, the turbulence intensity was set to 5% to depict medium to high turbulence experienced during fluid flow. Taking into considerations pipelines with curved local geometries, the turbulent intensity is great at this region due to mixing flow, and contributes to an increase in the rate of erosion, mechanical stress, pipe fatigue, deformation and damage at this area [10].

Frictional forces acting in the fluid-wall interface during crude oil transport can be detrimental to pipe structural integrity. The frictional force offers resistance to fluid flow and a constant reduction in the flow rate with time.

The term wall viscosity is synonymous to wall viscous drag, and can be defined to be the resistance to fluid flow offered by the wall surface against the moving fluid [12]. Wall viscosity is the measurable parameter and is measured in ppm (pounds per mass). Limited work has been undertaken in this area and successful achievement of the set objectives will add to the existing knowledge, in the area of fluid dynamics through a close media.

Transportation of crude oil is usually accompanied with a measurable amount of sand particles, water and associated gases [2, 3]. The contaminant solid particles exist as sand, insoluble scales, wax, minerals and other solid materials. The collision with the pipe wall surface impinges on the elbow surface, deforming or stripping away the surface material in a process known as erosion [4]. The gradual depletion of the corrosive-

resistant layer or chemical inhibitor exposes the pipe surface to chemical interaction with the corrosive fluid. The synergy effect is time-consuming and expensive, due to high maintenance cost and unplanned production stoppages [5]. It is important to identify measurable parameters that can be used to estimate the severity of the solid particles impingement in pipeline surfaces, to properly address this problem. Conventionally, the average erosion rate at the pipe elbow is used as a suitable parameter to understand the impact of sand presence in the transported fluid to the pipeline structural integrity [1, 5, 6].

Abdulla, (2011) performed a similar work on estimating rate of erosion due to the presence of contaminant particles. His investigation was conducted for three different cases, that is, water, oil and/or gas with sand transported separately. It was observed that the rate of erosion was predominant at the pipe elbow junction for all three cases [6]. Hence, there was no need to conduct the same research to identify the erosion hotpot. Fig. 1 shows erosion hotspot at the pipe elbow (junction point) for oil-gas and sand flow case scenario. Here, the maximum erosion rate recorded was 4.6807E-08 kg/m^{2}s using the E/CRC erosion model with STAR C++ software [6]. The difference between his work and this study is the introduction of a triple right angle pipe elbow connected by three longitudinal pipe sections. Also, the analysis on frictional wall viscosity due to fluid-wall interaction was considered. The above mentioned objective function was not conducted in his research.

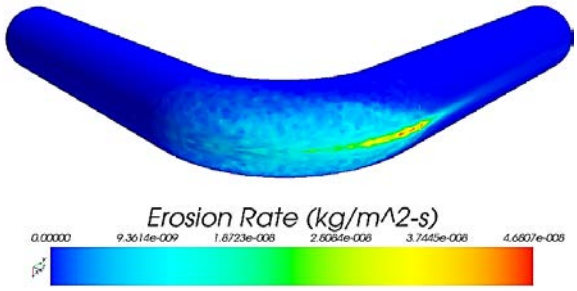

Figure 1: Erosion rate distribution at the pipe elbow during oil, gas and sand flow [6]

One of the objectives in this paper is to estimate the average erosion rate across a triple 90° (S-shaped) local pipe elbow and will address the missing link in his research to provide a better prediction. This is a novel research and very limited or no work has been done in this area.

Adding to the literature, AL-Baghdadi et al. (2017) investigated on erosion severity in a single pipe elbow during crude oil transport due to sand contamination. Observation of results validated the theory that the maximum erosion rate is experienced at the pipe elbow. This publication is recent and a number of missing links were identified. The scientific gap here are, no sensitivity studies on the effect of flow properties for the continuous and discrete phases were considered and a single pipe elbow was used as the model geometry. These scientific loops holes has created basis for further studies.

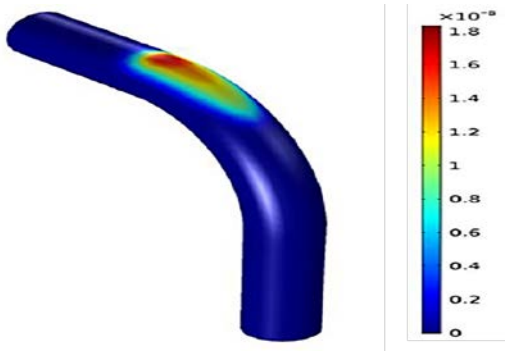

Figure 2: Erosion rate distribution during crude oil and sand flow [12]

2. SIMULATION METHODOLOGY

Computational Fluid Dynamics (CFD) Simulation involves the application of computers to produce quantitative and qualitative predictions and/or analysis of fluid flow behavior, which is based on the conservation laws such as conservation of mass, momentum, and energy. When properly implemented, CFD is efficient for flow physics and parametric studies that would be practically impossible to achieve with theoretical or experimental methods.

CFD simulations apply two dominant approaches, that is a finite difference and finite element simulations for which the latter is considered in this paper. In CFD study, the discretization of the spatial domain into grid points was performed. Matching of the numerical solution forward in discretization time steps was taken into consideration, to properly resolve fluid flow features at wall boundaries and flow media.

In the formulation of finite element or volume, the equations of motion are solved within the small grid elements that constitute the entire spatial flow domain with matching conditions between elements, which then leads to a systematic algebraic equation that can be solved numerically. The choice of discretization scheme depends on the prevailing flow conditions, for example, compressible and incompressible fluid flow. The prevailing flow condition adopted in this paper was the incompressible fluid flow, where the change in fluid density is not significant.

2.1 Pipe Model Design and Material Selection

The pipe design type was chosen to mimic pipelines installed to bypass an S-shape geographic terrain, connecting the petroleum production site to destination. COMSOL geomodeler was used in the design of the pipe model. The pipe model consist of three cylindrical section of length 10m, 3m and 3m arranged in series respectively. These sections are connected to each other by two elbow with 3m outer radius and curvature angle of 90°. A common radius 0.7m was considered in the design. Note that, these are hypothetical values used for analytic purposes, to mimic industrial flow processes. The model geometry can be seen in Fig. 3 below. The model material is made of steel of hardness 1.96E09 N/m^2. From vivid view of Fig. 3 (a) shows the pipe representation in 3D, showing both inlet and outlet sections. The figure at the right (b) of Fig. 3, shows a symmetric view of the pipe model with detailed dimension of each connected sections.

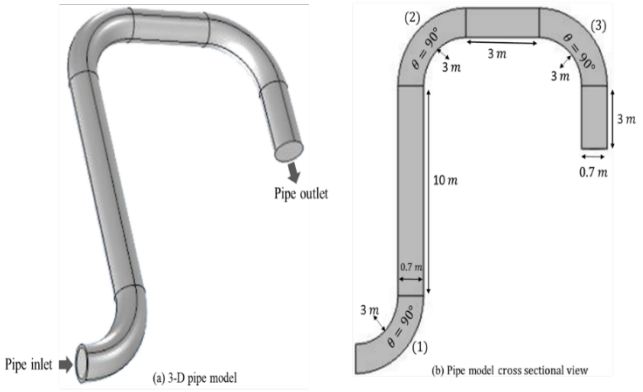

Figure 3: (a) 3-dimensional pipe model with triple 90° elbow and (b) pipe modelling dimensions

2.2 Pipe Model Meshing

Model meshing or mesh creation is the next pre-processing step after the model geometry has been created. This is a common practice when conducting CFD simulation, and thereafter, the boundary conditions are set to initiate flow of species through the transport media. BY definition, meshing is the discretization of the model geometry in to smaller elements, to create a flow domain and better resolve flows at sensitive areas.

There are mainly three (3) categories of meshing techniques. These are structured, unstructured and hybrid meshing. The choice of mesh type lies on the accuracy factor, complexity in the geometric shape of the geometry and type of physics to be selected. It is a common practice to generate an unstructured mesh for model design with a complex topology, due to its flexibility and reduced computation time. The main difference between the structured and unstructured meshes is the use of hexahedral elements, with implicit connectivity of points in the mesh, and tetrahedrons elements with an explicitly defined mesh connectivity respectively.

Due to the compromise in the solution accuracy with the unstructured meshing, most especially for elements in sensitive areas such as the wall boundary, a structured meshing is most suitable and was considered in the model meshing process. The model meshing can be seen in Fig. 4 (a) and (b) below.

Fig. 4(a) shows how the sweep option created a distributed hexahedral structured grid across the domain, while Fig. 4(b) is a symmetrical view of the model meshing, showing interior mesh and boundary layers.

Cite The Article: Chukwugozie Jekwu Ejeh, Gbemisola Precious Akhabue, Chigozirim Cyprian Onyekperem, Evans Boah Annan, Kingsley Kwaah Tandoh (2019). Evaluating the Impact of Unsteady Viscous Flow and Presence of Solid Particles on Pipeline Surfaces During Crude Oil Transport Using Computational Fluid Dynamics Analysis. *Acta Mechanica Malaysia, 2(2): 20-27.*

The creation of boundary layers is critical in Computational Fluid Dynamics studies. This is because, parameters measured at the wall boundary are sensitive to changes in flow gradient, and it is important to ensure that the mesh structure is fine in this area with y^+ value less than 1, most especially when using the two-equation $k-\omega$ turbulent model in the CFD simulation.

The decision on the final mesh design was based on the mesh sensitivity plot described in the Section 2.1.1.1 below. The choice of the best mesh design lies within the convergence range.

2.2.1 Mesh Sensitivity Analysis

Mesh sensitivity is an important process that should be considered in the selection of the best meshing strategy. This involves, increasing the meh size and observing how it affect the accuracy of prediction, of the objective results. From literature, it was established that fine mesh provide a more accurate prediction of the solver solution than a coarse mesh. The Figures 5 and 6 shows the mesh sensitivity plots for drag force (wall viscous force) and velocity magnitude predictions for various element size considered. The plots describe how both quantities converge after a total of 27,000 elements. The number of elements considered in the final mesh design was composed of 55, 381 elements. Details for the final mesh design strategy can be seen in Table 1 below.

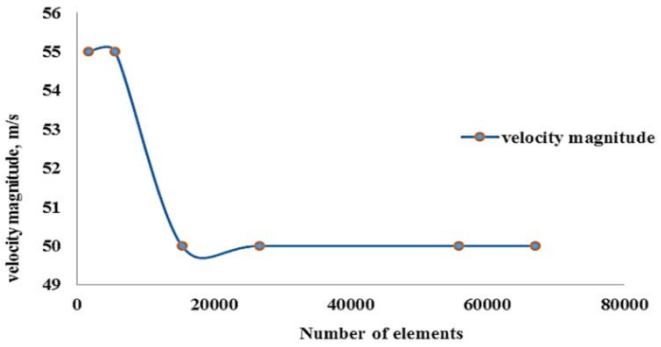

Figure 4: mesh sensitivity plot of velocity magnitude predictions with number of elements

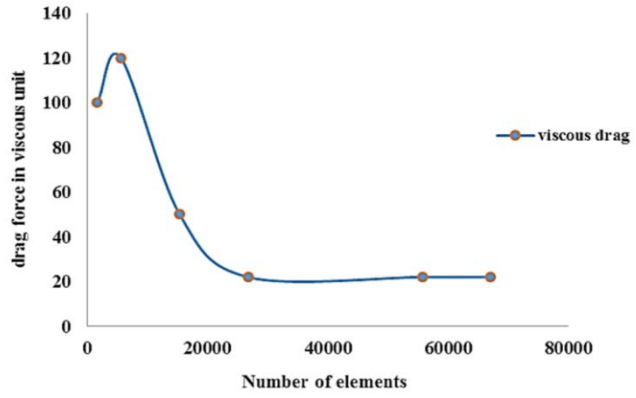

Figure 5: mesh sensitivity plot of drag force predictions with the number of elements

Table 1: Final mesh design parameters

Parameters	Values
Meshing type	Structured mesh
Maximum element size	0.207
Minimum element size	0.0619
Curvature factor	0.4
Maximum element growth rate	1.15
Number boundary elements	20
Physics / Method	Fluid Dynamics
Number of elements	55,831
Face meshing method	Quadrilateral (generate hexahedra)

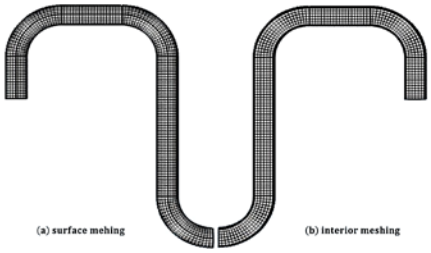

Figure 6: (a) pipe surface mesh design and (b) interior mesh design

2.3 Fluid Type and Properties

The Table 2 below contains important fluid data used in the material section during the simulation setup. The Bonny light crude type was used as the case fluid just for analytic purposes. Amongst the family of fluid properties, density is the most important for this investigation. Abdulla, (2011) showed that, a change in the density of fluid has an influence on the prediction of average erosion rate. This is based on the fact that the greater the fluid gravity, the lower the momentum energy of the discrete phase (solid particle) during transport.

Table 2: Bonny light crude properties

Parameters	Values
Crude Oil Type	Bonny Light
API Gravity	35.4 ° API
Kinematic Viscosity at 50 °C	2.9 mm^2/s
Crude Oil Density	847.8 kg/m^3
Chemical formula (n-octane)	C_8H_{18}

2.4 Physics Selection and Boundary Conditions

In this study, solid particles were assumed to be present in the produced transported fluid as the suspended phase, whiles the case fluid served as the continuous phase. Table 3 below details of the boundary conditions considered in the simulation setup for both turbulent model and particle tracing physics.

Table 3: Boundary conditions and Discretization Scheme data

Parameters	Values
Initial velocity	40 m/s
Initial temperature	293.15 K
Pressure at outlet	0 Pa
Particle density	0.154 kg/m^3
Particle flow rate	0.6 Kg/h
Particle diameter	1.13E-04
Particle type	Solid
Particle specific heat capacity	2200 J/kg*K
Particle latent heat	42000 J/kg
Initial particle temperature	293.15 K
Particle mass flow rate	1.56 kg/h
Number of particles per release	5000
Wall type	No Slip
Wall treatment	Wall functions
Turbulent dissipation model	Discrete random walk
Flow type	Fully developed incompressible flow
Turbulence model type	Reynolds-Average Navier Stokes (RANS)
Turbulent model	Two equation, $k-\omega$ model

2.5 Computational Fluid Dynamic Modelling

2.5.1 Continuous Phase modelling

A multiphase flow system is any system consisting of more than one phase present in the transmission media. An example is gas, liquid, bubbles and/or solids. In multiphase modelling, gas or liquid are considered as the continuous phase, whiles bubbles and particles exit as a suspended or discrete phase. In this work, the multiphase flow system was composed of crude oil (n-octane), water and solid particles. Here, the liquid and water

Cite The Article: Chukwugozie Jekwu Ejeh, Gbemisola Precious Akhabue, Chigozirim Cyprian Onyekperem, Evans Boah Annan, Kingsley Kwaah Tandoh (2019). Evaluating the Impact of Unsteady Viscous Flow and Presence of Solid Particles on Pipeline Surfaces During Crude Oil Transport Using Computational Fluid Dynamics Analysis. *Acta Mechanica Malaysia, 2(2): 20-27.*

was set to be the continuous phase, whiles the solid particle existed as the suspended phase. This best describe a typical oil and gas flow through pipelines with the presence of contaminant particles.

Computational methods rely on the use of mathematical models to analyse systems. For fluid flow modelling, the mathematical model used to govern flow through a media, are based on the conservation law. This law includes the conservation of mass, momentum and energy. The Navier-Stokes equation is an example of a flow equation that rely on the conservation principle. The equations (1), (2) and (3) below represents the conservation of mass, momentum and energy equation.

$$\frac{\partial(\rho_i \alpha_i)}{\partial t} + \nabla.(\rho_i \alpha_i V_i) = 0 \quad (1)$$

The first and second term in equation 1 above represents the rate of change in density-rate of mass and the net rate of mass of the continuous phase. Where α is the volume fraction which must be equal to 1 in the fluid cell (single phase), i is the number of phase (liquid, gas and solid) present in the element and ∇ is the partial derivative of quantity in all directions [6].

The conservation of momentum equation is based on Newton's second law which states that, the rate of change of momentum of the fluid particle is equal to the sum of all forces acting on the particles [6].

$$\frac{\partial(\rho_i \alpha_i V_i)}{\partial t} + \nabla.(\rho_i \alpha_i V_i V_i) = -\alpha_i \nabla_p + \nabla.[\alpha_i(\tau_i + \tau_i{}^t)] + \rho_i \alpha_i g + M_i \quad (2)$$

Where τ_i represents the molecular stress, $\tau_i{}^t$is the turbulent stress and M_i is the interphase momentum exchange acting per unit volume. It should be noted that the interphase momentum equation is the sum of the virtual mass force, drag force, lift force and turbulent dispersion force [6].

The combined conservation of mass and momentum equation are known as the Navier-Stokes equation. The conservation of energy equation was developed from the first law of thermodynamics which states that the rate of change of a particle equals the rate of heat added to the particle and the rate of work done on the fluid particle. The energy consevation equation is shown below.

$$\frac{\partial(\rho E)}{\partial t} + \nabla.\left(V(\rho E + p)\right) = \nabla.\left[k_{eff}\nabla_t - \sum_j h_j J_j + (\bar{\bar{\tau}}_{eff}.V)\right] + S_h \quad (3)$$

From the equation (3) above, there are four (4) terms which constitute the entire model equation. The first term is the heat transfer due to conduction or diffusion whiles the second term represents the fluid diffusion heat transfer. The subsequent term represents heat loss due to viscous dissipation and the last term includes other sources such as radiation.

2.5.2 Dispersed Phases Modelling

Some of the approaches used in the modelling of multiphase flow system with CFD, is the Eulerian model, Lagrangian model, and Volume of Fluid Model (VOF) [6]. Fundamentally, the Eulerian model, Lagrangian model, and VOF model are used to model gas flow, gas-solid flow and liquid-gas-solid respectively.

In this study, the Volume of Fluid (VOF) model was used based on the above selection criteria. Here, a set of momentum equation solves for all phases and volume fractions in each grid cell within the flow domain and assumes that the velocity, pressure, and temperature of all phases remain static [6]. The volume fraction is zero (0) in cells with no fluid and one (1) in cells filled with fluid.

2.5.3 Particle Tracing and Drag Force Modelling

Newton's law of motion fundamentally governs the movement of a body under the influence of unbalanced external forces. In this study, particle motion in fluids is governed by Newton's law [11, 12]. It can be expressed mathematically as shown below:

$$\frac{d(m_p V)}{dt} = F_D + F_g + F_{ext} \quad (4)$$

where m_p is the particle mass in kg, v is the particle velocity in m/s, F_g is the gravitational force in Newton F_D is the drag force in Newton, and F_{ext} is an external force sourced from the kinetic energy of the continuous phase in Newton.

Drag force existing at the fluid-wall interphase can be modeled using the equation below [11, 12]. The model equation is a function of fluid velocity gradient, viscosity at the interface, pipe diameter and density.

$$F_D = \frac{1}{\tau_p} m_p (V - U) \quad (5)$$

$$\tau_p = \frac{\rho_p d^2{}_p}{18\mu} \quad (6)$$

$$V = u + \Delta u, \text{ where } \Delta u = \delta\sqrt{\frac{2k}{3}} \quad (7)$$

where τ_p is the response time for a particle in motion measured in seconds, V is the instantaneous flow velocity in the drag force, m/s, k is the turbulent kinetic energy, δ is the vector uncorrelated Gaussian numbers with unit variance.

2.6 Segregated Solver Analysis

The segregated solver is an essential computational tool in COMSOL Multiphysics software which solves the turbulent model composed of velocity, pressure and turbulent intensity variable iteratively, until the solutions to the variables converge to an acceptable error limit. This solver work differently from the fully coupled approach, which is based on the Newton Raphson iteration method. Here, the segregated solver de-couples all equations (conservation of momentum, energy and mass equation) making it easier to solve for velocity, pressure, and turbulence [13].

The segregated solver is reliable and requires less memory than the fully coupled solver. The Fig. 5 below is the process algorithm that demonstrates how the segregated solver in COMSOL Multiphysics works with associated governing equations.

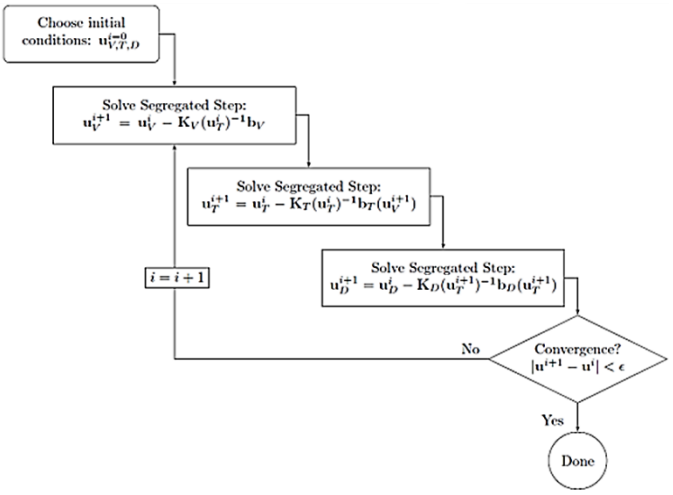

Figure 7: segregated solver process algorithm [8]

The plot shown in the Fig. 6 below demonstrates the solver convergence. It vividly informs that, the error of estimation in the solver predictions for velocity, pressure and turbulence variables converges after 80 iterations. The estimated solution iterative error lie in the interval $10^{-2} - 10^{-4}$. This error margin is within the acceptable limit.

Note that, in the solver settings, the convergence criteria was reduced to 1E-10 tolerance level, to allow the variables to converge. This analysis was conducted to validate the model and to ensure that the solution converges with an acceptable error margin.

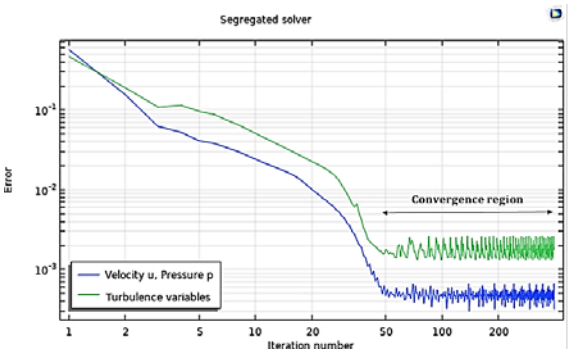

Figure 8: Plot showing error of estimation and solver convergence with iteration

The segregated solver used approximately 51 minutes, 32 seconds computational time for the solution to converge. It should be noted that

the computational time varies with the CPU processing power and the computer used to run this simulation Random Access Memory was 4GB.

2.7 Time-Dependent Solver Analysis

A time-dependent solver is usually applied when studying time-dependent processes. For nonlinear problems such as particle tracing in the fluid system, the time-dependent solver solves all nonlinear system of equations for each time step through a set of iterative processes. This iterative process is based on the Newton-Raphson technique. This technique evaluates each function and its derivatives at every given time step. The derivative is commonly referred to as the Jacobian, and is associated with high computational cost. In this case, the software package attempt to minimize the error of estimation by re-evaluating the Jacobian, by default. As a result, it becomes difficult for the solver to converge.

Comparing Fig. 9(a) and (b), the time-dependent solver solution was unable to converge even after 500 iterations (See Fig. 9(a)) due to the restrictions in the solver relative tolerance. The relative tolerance was reduced from 1E-03 to 1E-10 significant figures, to allow the solution to settle at a frequency of 100 after the minimum iteration value of 10 (See Fig. 9(b)). This implies that, when conducting a time-dependent study, it is important to reduce the relative tolerance value to about ten (10) significant figures, to allow the solution to converge.

The total computational time for the second simulation run was 37 minutes, 9 seconds on average for fluid velocity set at 40 m/s. Compared to the segregated solver plot in Fig. 8, it took less computational time for the time-dependent solver to converge to the exact solution. This is because, the segregated solver is required to decouple the velocity and pressure equation to compute for velocity, pressure field, and turbulence variable.

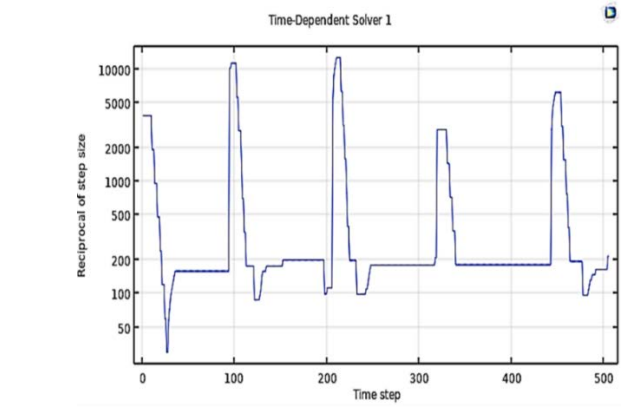

Figure 9a: time-dependent solver plot showing how the solution diverges with time steps

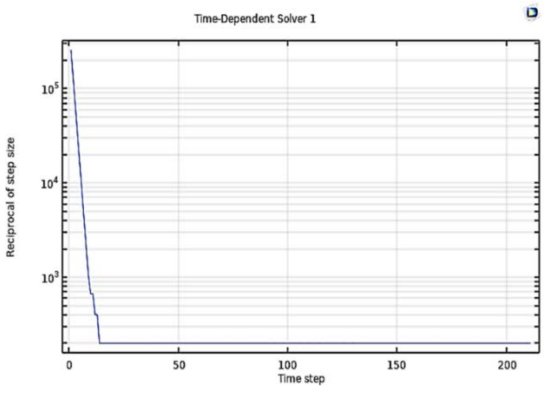

Figure 9b: time-dependent solver plot showing how the solution converges with time steps

3. RESULTS AND DISCUSSION

The results displayed in this section are concerned with the flow variables used in this study, to understand the fluid dynamic behavior. In the analysis of fluid flow, it is important to consider velocity magnitude and pressure predictions within the flow domain. The Figures 10 and 12 shows variations in fluid velocity and pressure respectively across the flow domain. From a critical observation of Fig. 11, it can be observed that mixing flow occurs at local geometries with steep curvature. That is at the 90° pipe elbow sections. At this point, the turbulent intensity and fluid velocity predictions are higher than the set maximum values in the inlet boundary condition. In the case of velocity, the maximum fluid velocity at the boundary inlet was 40 m/s. From further observation, the velocity magnitude predictions at this mixing point read a value of 50 m/s at the elbow number (1) and (2). This phenomenon is based on the Brownian principle, which describes the erratic motion of fast-moving particles in a fluid due to continuous bombardment with molecules in its surrounding.

In addition, from critical observation of Fig. 10 (right) the fluid flow velocity magnitude profile is not centralized, but skewed to the right and attaches itself to the pipe wall. This implies that the fluid flow is higher around the walls than other sections. This is due to the Coanda effect and it describes the tendency of the fluid to attach itself to a convex shaped surface and remains attached even when the surface curvature has been modified [18].

It should be noted that the velocity magnitude of the crude oil was observed to be maximum at the steep sections of the model geometry. This is due to the influence of the Coanda effect.

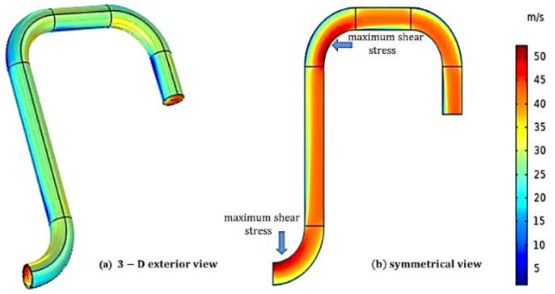

Figure 10: velocity magnitude contour plot across the pipe cross-section

From Fig. 11 below, the flow mixture is intense at the elbow section than other regions. This is as a result of recirculation of fluids when it comes in contact with a convex structure. By so doing, solid particles in the fluid will experience multiple collisions with the elbow surface.

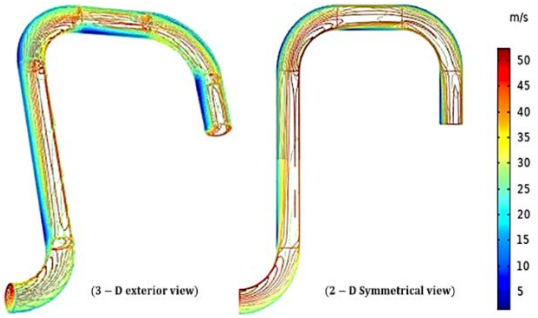

Figure 11: Contour plot showing flow mixture and re-circulation at pipe curvatures

The stress exerted at this local geometry can be evaluated from static pressure values predicted at this region. Fig. 12 below is a contour plot showing fluid static pressure predictions across the flow domain. It can be observed that, the maximum static pressure is of magnitude 5.6×10^5 Pa. This value is significant and may contribute to wall lift-off in a typical industrial setting. The pressure prediction was found to be dominant at areas just after the curve path.

It was deduced that the fluid static pressure is higher at regions with lower velocity magnitude. At this area, the fluid is said to recirculate and detached, giving rise to a stagnation point.

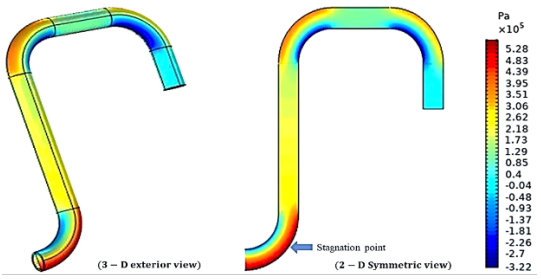

Figure 12: profile of fluid pressure across the flow domain

4. ANALYSIS OF VISCOUS DRAG TO FLOW RESISTANCE

Viscous drag in a pipe is a common phenomenon experienced when the continuous phase flows relatively with a solid surface in contact. In this case, the solid surface represents the pipe wall, and the wall condition was set as a slip boundary.

To understand the effect of this relative motion and friction on the pipe wall, wall viscosity which is a function of drag force was used in this paper as the measurable parameter. The relative motion between the transported fluid and pipe wall induces shear stress across the pipe. This can be visualized using wall resolution in the viscous unit. From a scientific point of view, this parameter is dependent on certain fluid properties such as fluid dynamic viscosity, velocity, temperature and density [12]. Here, analysis of the effect of temperature was indirectly introduced in the simulation, when a change in the dynamic viscosity was considered. This is because, a change in the viscosity of fluids is directly proportional to temperature change [12].

4.1 Effect of Variable Fluid Dynamic Viscosity

In this paper, the effect of crude oil dynamic viscosity to flow was investigated. The dynamic viscosity value was varied between 0.08 to 0.20 Pa.s whiles keeping the fluid density and temperature constant. That is 848 kg/cu.m and 40 m/s respectively. These parametric values were varied based on the theory that the dynamic viscosity of a fluid is affected by changes in temperature. As such, an increase in fluid temperature will cause a reduction in the viscosity of fluids [13, 14].

From Fig. 13 below, it is obvious that the wall viscosity is affected by changes in the crude oil dynamic viscosity. An increase in dynamic viscosity yielded a reduction in the wall viscosity predictions. This signifies that the wall temperature is increasing due to the friction at contact areas. A maximum of 1.5×10^8 ppm wall viscosity was obtained at fluid viscosity equal to 0.12 Pa.s. Regions with a red colour band are interpreted to be the hotpost exposed to maximum frictional contact with the moving fluid. It has been identified with an arrow and can be seen in Fig. 13(a).

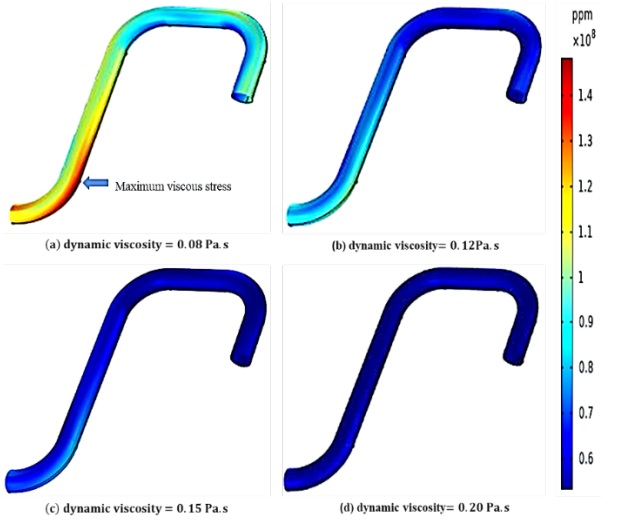

Figure 13: Effect of fluid dynamic viscosity to pipe wall viscous resolution

4.2 Effect of Variable Fluid Velocity

The velocity of a fluid is also an important factor for consideration. The driving force present in the reservoir energizes the fluid and maintains the flow rate for a period of time through the production pipes. Flow in most conventional reservoirs is unsteady due to reservoir heterogeneities. As such, the velocity of the fluid is affected. To better understand the influence of changes in the flow rate on the pipe wall viscosity, the velocity of crude oil was varied at the inlet boundary section in the range 10 to 60 m/s. This values are hypothetical and are considered for analytic purposes. The dynamic viscosity was kept constant at 0.58 Pa.s and a fluid density of 848 kg/cu.m.

Results shown in Fig.14 below shows that an increase in the velocity magnitude induced an increment in the wall viscosity prediction. Predicted values peaked at 2.2×10^8 ppm at velocity magnitude within 50 to 60 m/s and it was located at the area closest to the inlet shown in Fig. 14(e) and (f)

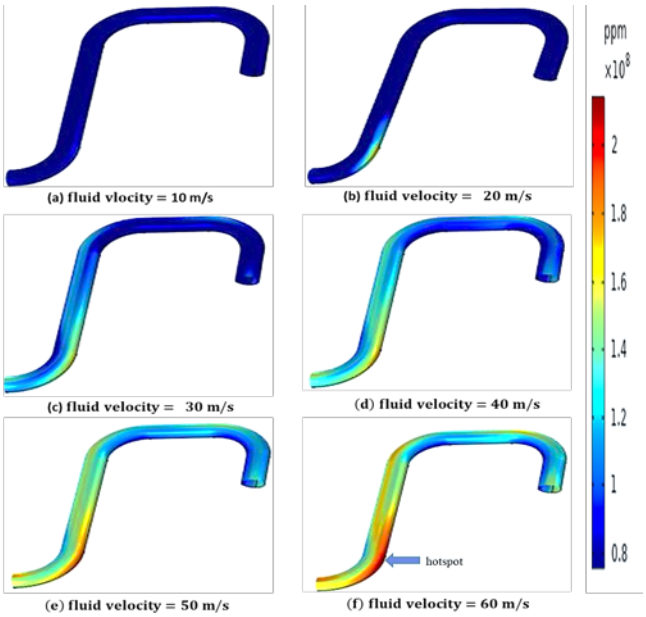

Figure 14: effect of variable velocity to pipe wall viscous resolution

4.3 Effect of Variable Fluid Specific Gravity

The density of fluid is another important parameter that can affect the wall viscous resolution. From theoretical concepts of frictional forces in pipes, the frictional force is affected by the mass of the continuous phase [15, 16]. Friction force and mass of fluid vary directly proportional to the mass of fluid. Density is the ratio of the mass of a substance to the volume. This means that, an increase in the density of crude oil will cause a proportional change in wall viscosity. This theory was proven from the results obtained in Fig. 15 below. Results showed that, as the density of crude oil was increased, the wall viscosity predictions increased significantly. A maximum wall viscosity of 2.1×10^8 ppm was predicted. Hence, the heavier the fluid the higher the degree of frictional contact between the pipe wall and fluid (crude oil) in transport. The arrow in Fig. 15 (d) shows areas with maximum wall viscosity during oil flow. Here, two hotspots are identified.

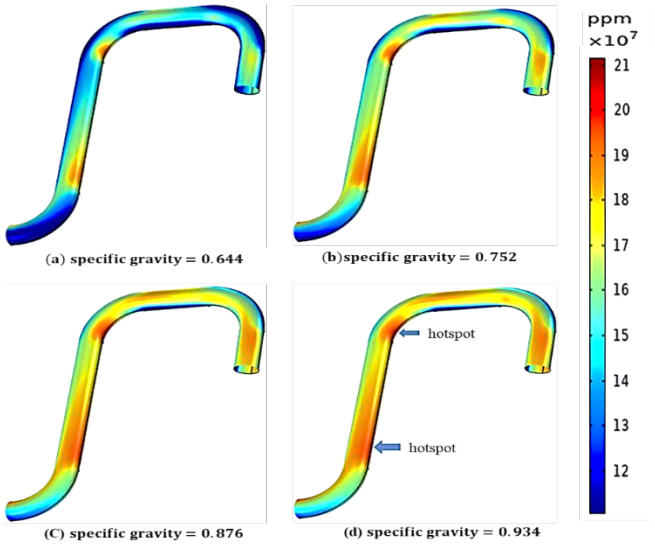

Figure 15: effect of fluid specific gravity to pipe wall viscous resolution

4.4 Analysis of Viscous Stress on Pipe Wall

Viscous drag between fluids and wall in relative motion exert stress on the pipe. The Fig. 16 below shows the magnitude of stress exerted on the pipe wall due to frequent interaction of the crude oil with the pipe surface during transport. A maximum stress reading of magnitude 0.6×10^4 N/m^2 was predicted at the identified hotspots. This viscous stress value is significant but does not exceed the fracture or yield strength for pipeline made of steel. The result in Fig. 16 was obtained at dynamic viscosity of 0.08 Pa.s, the fluid velocity of 60 m/s and specific gravity 0.934. These data represent optimum results obtained from section 4.1.1, 4.1.2 and 4.1.3 respectively.

Cite The Article: Chukwugozie Jekwu Ejeh, Gbemisola Precious Akhabue, Chigozirim Cyprian Onyekperem, Evans Boah Annan, Kingsley Kwaah Tandoh (2019). Evaluating the Impact of Unsteady Viscous Flow and Presence of Solid Particles on Pipeline Surfaces During Crude Oil Transport Using Computational Fluid Dynamics Analysis. *Acta Mechanica Malaysia, 2(2): 20-27.*

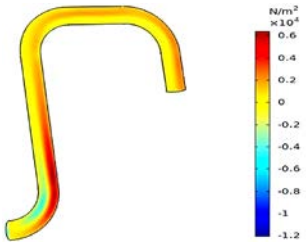

Figure 16: viscous stress in the pipe during crude oil transport

4.5 Analysis of Frictional Velocity on Pipe wall

It was established in this work that, frictional force existed between the pipe wall and moving fluid. This was based on the wall viscosity predictions. The unsteadiness in the viscosity of crude oil at wall boundary contributed to an uneven distribution in viscous stress and drag across the pipe wall. This can be visualized in Fig. 16 and Figures 13 – 15 respectively.

Further study was conducted to estimate frictional velocity throughout the pipe geometry. This was aimed at to estimate the reduction in velocity of crude oil at the fluid-wall contact, using frictional velocity as the measurable parameter.

The Fig. 17 below provides critical information about the magnitude of reduced fluid velocity due to wall viscosity. A maximum frictional velocity magnitude of 3.4 m/s velocity was predicted at the hotspot. This informs that, flow restrictions due to high frictional force is experienced at the boundary layer, than outer parts of the flow media.

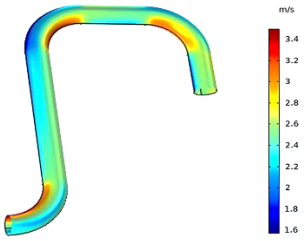

Figure 17: wall frictional velocity across the pipe surface

5. ESTIMATION OF AVERAGE EROSION RATE

In this study, the presence of particles in the continuous phase was considered. This section is concerned with sensitivity studies of the influence of fluid density, particle diameter and mass flow rate to average erosion rate prediction. The shape of the particle considered in this work is an isotropic sphere.

5.1 Influence of Crude Oil Density

Different erosion models were used to estimate the average erosion rate whiles taking into consideration a change in the density of crude oil. The Finnie, E/CRC, Oka, et al and DNV model was used in this study. Fig. 18 shows how crude oil density affects erosion rate prediction. From observation, the DNV model predicted higher values of erosion rate.

It is obvious that, when the density of crude oil was varied from 808.9 - 879.16 kg/m^3 (density for different crude type), the average predicted rate of erosion decreased proportionally. This confirms results obtain by Abdulla, (2011), and Al-Baghdadi et al. (2017). The maximum average erosion rate achieved was 2.35E-06 kg/m^2s using the DNV erosion model.

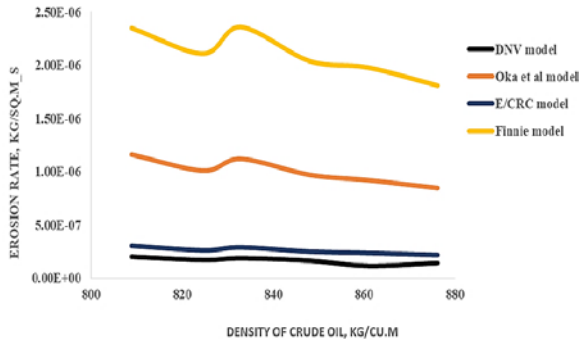

Figure 18: Effect of crude oil density to the average rate of erosion

Table 4: below is a summary of the erosion rate predictions using the various erosion models. It was observed that, higher predictions of average erosion rate were achieved with the DNV model as predicted by Abdulla, (2011) compared to others.

Table 4: Effect of crude oil density on average erosion rate predictions

Crude Oil Density, (kg/m^3)	DNV model, (kg/m^2s)	Oka et al model, (kg/m^2s)	E/CRC model, (kg/m^2s)	Finnie model, (kg/m^2s)
876.16	1.81E-06	2.17E-07	8.46E-07	1.41E-07
860.8	1.98E-06	2.36E-07	9.20E-07	1.15E-07
848.0	2.04E-06	2.49E-07	9.70E-07	1.63E-07
832.9	2.36E-06	2.88E-07	1.12E-06	1.86E-07
824.6	2.11E-06	2.61E-07	1.01E-06	1.69E-07
808.9	2.35E-06	3.03E-07	1.16E-06	2.01E-07

5.2 Influence of Particle Mass Flow Rate

Similarly, the effect of particle size was also investigated. Here, the average velocity, dynamic viscosity and density of the fluid material was set to 40 m/s, 0.54 Pa.s and 848 kg/m^3 at the boundary conditions respectively. It was necessary to maintain these variables whiles varying the particle mass flow rate. The particle mass flow rate value used in this study ranged between 0.1 – 2.6 kg/h. These variations was effected at the physics boundary condition.

From the results shown in Fig. 19, it was found that, when the particle mass flow rate was increased, the average erosion rate also increased. This is based on the concept that, when the kinetic energy of the moving solid particles, the greater the impact force at the pipe wall. Hence, the rate of wall erosion is expected to increase.

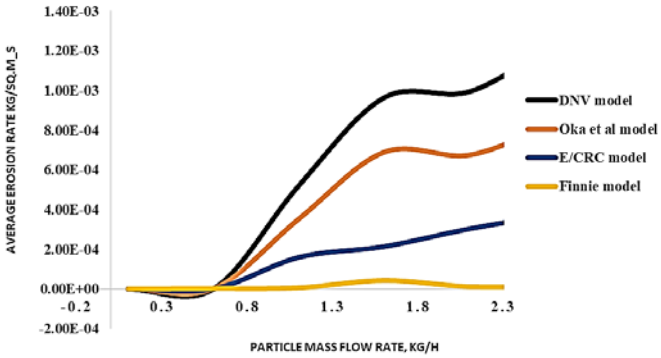

Figure 19: Effect of particle mass flow rate to average erosion rate

From Table 5, the maximum average erosion rate predicted in this case study was 1.23E-03 kg/m^2s, 8.85E-04 kg/m^2s, 3.75E-04 kg/m^2s and 1.37E-05 kg/m^2s using DNV, Oka, et al., E/CRC and Finnie model respectively. Obviously, all implemented erosion models yielded different predictions of average in section 5.1.1, 5.1.2 and is expected to be the same for the case in section 5.1.3.

Table 5: Effect of Particle mass flow rate on average erosion rate predictions

Particle Mass Flow Rate, (kg/h)	DNV model, (kg/m^2s)	Oka et al mo1del, (kg/m^2s)	E/CRC model, (kg/m^2s)	Finnie model, (kg/m^2s)
0.1	2.53E-08	1.53E-07	3.95E-08	3.25E-07
0.6	1.63E-07	9.70E-07	2.90E-07	2.04E-06
1.1	5.21E-04	3.53E-04	1.59E-04	5.80E-06
1.6	9.64E-04	6.89E-04	2.13E-04	4.29E-05
2.1	9.94E-04	6.74E-04	3.03E-04	1.10E-05
2.6	1.23E-03	8.85E-04	3.75E-04	1.37E-05

5.3 Influence of Particle Diameter

Lastly, the effect of particle diameter was considered in this research. This was considered because in real life cases, the solid particles transported as a suspended phase do not have a fixed diameter. Hence it was vital to perform this analysis.

Cite The Article: Chukwugozie Jekwu Ejeh, Gbemisola Precious Akhabue, Chigozirim Cyprian Onyekperem, Evans Boah Annan, Kingsley Kwaah Tandoh (2019). Evaluating the Impact of Unsteady Viscous Flow and Presence of Solid Particles on Pipeline Surfaces During Crude Oil Transport Using Computational Fluid Dynamics Analysis. *Acta Mechanica Malaysia, 2(2): 20-27.*

The particle diameter was varied within the range of 0.7 – 3.210^{-4} m. This is a hypothetical range of values used to perform this sensitivity study. Results obtained shows to be interesting where the maximum erosion rate was achieved at particles diameter between 1.0 10^{-4} m and 1.510^{-4} m, and showed lower readings after this range of values. It should be noted that fluid properties kept constant in the previous study also applies to this study. Adding to this, the particle mass rate was kept constant at 0.6 kg/h.

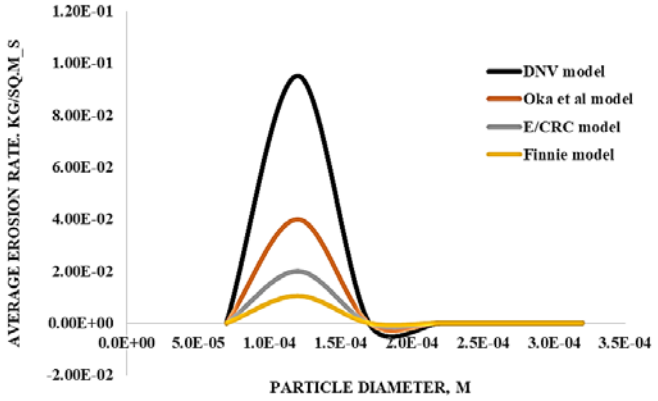

Table 6 below gives a detail report of discrete values predicted for different erosion models.

Predicted values of average maximum erosion rate using DNV, Oka, et al., E/CRC and Finnie models are 9.51E-02 kg/m^2s, 3.99E-02 kg/m^2s, 2.00E-02 kg/m^2s and 1.05E-02 kg/m^2s.

Table 6: Effect of Particle diameter on average erosion rate prediction

Particle Diameter, (10^{-4} m)	DNV model, (kg/m^2s)	Oka et al model, (kg/m^2s)	E/CRC model, (kg/m^2s)	Finnie model, (kg/m^2s)
0.7	2.48E-08	2.65E-08	7.08E-09	2.43E-08
1.2	9.51E-02	3.99E-02	2.00E-02	1.05E-02
1.7	1.22E-09	2.07E-09	3.02E-10	1.08E-09
2.2	7.58E-10	2.17E-09	6.37E-10	1.40E-11
2.7	4.40E-09	1.10E-08	6.40E-10	7.82E-10
3.2	1.31E-11	5.65E-11	1.43E-11	1.12E-11

6. CONCLUSION

It was concluded that unsteady viscous flow indeed has an influence on the wall viscosity and viscous stress across the pipe geometry. An increase and decrease in the velocity, specific gravity and dynamic viscosity of crude oil respectively yielded increasing predictions in wall viscosity or wall resistance to flow. In addition, potential hotspots areas with a high prediction of frictional velocity and viscous stress were identified at the curved local geometry compared to other areas across the pipe geometry.

Studies on average erosion rate prediction using various erosion models showed that, when the particle mass flow rate and crude density was increased, the rate of erosion of the pipe increased significantly. All erosion models predicted different values of average erosion rate and this prediction correlates well with published works.

RECOMMENDATION

It is recommended that further study should be conducted to investigate the influence of the curvature angle of the pipe elbow to the rate of erosion and wall viscosity resolution.

CONFLICT OF INTEREST

We affirm that there is no conflict of interest and this is a collaborative work, agreed upon and submitted for publication.

REFERENCES

[1] Sanni, S.E., Olawale, A.S., Adefila, S.S. 2015. Modeling of sand and crude oil flow in horizontal pipes during crude oil transportation. Journal of Engineering.

[2] Das, G.S., Khanna, A.S. 2004. December. Parametric study of CO2/H2S corrosion of carbon steel used for pipeline application. In proceedings to the International Symposium of Research Students on Materials Science and Engineering.

[3] Islam, M.A., Farhat, Z.N. 2014. Effect of impact angle and velocity on the erosion of API X42 pipeline steel under high abrasive feed rate. Wear, 311(1-2),180-190.

[4] Parsi, M., Najmi, K., Najafifard, F., Hassani, S., McLaury, B.S., Shirazi, S.A. 2014. A comprehensive review of solid particle erosion modeling for oil and gas wells and pipelines applications. Journal of Natural Gas Science and Engineering, 21, 850-873.

[5] Okonkwo, P.C., Mohamed, A.M. 2014. Erosion-corrosion in the oil and gas industry: a review. Int. J. Metall. Mater. Sci. Eng, 4(3), 7-28.

[6] Abdulla, A. 2011. Estimating erosion in oil and gas pipeline due to sand presence.

[7] White, F.M. 1999. Fluid Mechanics, McGraw-Hill.

[8] Anderson, J.D., Wendt, J. 1995. Computational fluid dynamics (Vol. 206). New York: McGraw-Hill.

[9] Oliveira, G.M., Negrão, C.O.R. 2015. The effect of compressibility on flow start-up of waxy crude oils, J. Nonnewton. Fluid Mech. 220, 137–147. doi:10.1016/j.jnnfm.2014.12.010.

[10] Kumar, L., Zhao, Y., Paso, K., Grimes, B., Sjöblom, J., Lawrence, C. 2015. Numerical Study of pipeline restart of weakly compressible irreversibly thixotropic waxy crude oils, AI. 61, 2657–2671. doi:10.1002/aic.14844.

[11] Al-Baghdadi, M.A., Resan, K.K., Al-Waily, M. 2017. CFD investigation of the erosion severity in 3D flow elbow during crude oil contaminated sand transportation. Engineering and Technology Journal, 35(9 Part (A) Engineering), 930-935.

[12] White, F.M., Corfield, I. 2006. Viscous fluid flow (Vol. 3, pp. 433-434). New York: McGraw-Hill.

[13] Sparks, D., Smith, Cruz, V., Tran, N., Chimbayo, A., Riley, D., Najafi, N. 2009. Dynamic and kinematic viscosity measurements with a resonating microtube. Sensors and Actuators A: Physical, 149(1), 38-41.

[14] Davidson, M.R., Nguyen, Q.D., Chang, C., Rønningsen, H.P. 2004. A model for restart of a pipeline with compressible gelled waxy crude oil, J. Nonnewton. Fluid Mech. 123, 269–280. doi:10.1016/j.jnnfm.2004.09.007.

[15] Taitel, Y., Bornea, D., Dukler, A.E. 1980. Modeling flow pattern transitions for steady upward gas-liquid flow in vertical tubes. AIChE Journal, 26(3), 345-354.

[16] Bannwart, A.C. 2001. Modeling aspects of oil-water core-annular flows. Journal of Petroleum Science and Engineering, 32(2-4), 127-143.

Cite The Article: Chukwugozie Jekwu Ejeh, Gbemisola Precious Akhabue, Chigozirim Cyprian Onyekperem, Evans Boah Annan, Kingsley Kwaah Tandoh (2019). Evaluating the Impact of Unsteady Viscous Flow and Presence of Solid Particles on Pipeline Surfaces During Crude Oil Transport Using Computational Fluid Dynamics Analysis. *Acta Mechanica Malaysia, 2(2): 20-27.*